

## Supporting Information

### **Ambient-Air-Stable Li<sub>3</sub>InCl<sub>6</sub> Electrolyte with High Voltage Compatibility for All-Solid-State Batteries**

*Xiaona Li, <sup>a†</sup> Jianwen Liang, <sup>a†</sup> Jing Luo, <sup>a</sup> Mohammad Norouzi Banis, <sup>a, b</sup> Changhong Wang, <sup>a</sup> Weihan Li, <sup>a, c</sup> Sixu Deng, <sup>a</sup> Chuang Yu, <sup>a</sup> Feipeng Zhao, <sup>a</sup> Yongfeng Hu, <sup>a, b</sup> Tsun-Kong Sham, <sup>a, c</sup> Li Zhang, <sup>d</sup> Shangqian Zhao, <sup>d</sup> Shigang Lu, <sup>d</sup> Huan Huang, <sup>e</sup> Ruying Li, <sup>a</sup> Keegan R. Adair, <sup>a</sup> and Xueliang Sun<sup>\*a</sup>*

#### **Experimental Procedures**

**Preparation of the Li<sub>3</sub>InCl<sub>6</sub> SSE through ball milling route (ball milled-Li<sub>3</sub>InCl<sub>6</sub>):** Lithium chloride (LiCl, Alfa Aesar, 99.9%) and indium chloride (InCl<sub>3</sub>, Alfa Aesar, 99.99%) were weighed to the stoichiometric molar ratio. The mixtures were mechanically mixed in a ZrO<sub>2</sub> pot with ZrO<sub>2</sub> balls ( $\phi = 5$  and 10 mm, the mass ratio of balls to mixtures was 40). The mixing process was performed using a planetary ball milling apparatus at 500 rpm for 24 h. All the preparation processes were carried out with an Ar atmosphere.

**Preparation of the Li<sub>3</sub>InCl<sub>6</sub> SSE through annealing route (annealed-Li<sub>3</sub>InCl<sub>6</sub>):** Several hundreds of milligrams of the ball-milled Li<sub>3</sub>InCl<sub>6</sub> was pelletized at 200 MPa, sealed in a glass tube at ~10 Pa under vacuum, annealed at 260-400 °C for different duration (2-12 hours), and cooled to room temperature in 2 hours. All the preparation processes were carried out in an Ar atmosphere.

**Characterizations:** Powder X-ray diffraction (XRD) patterns were collected on a Bruker AXS D8 Advance with a Cu K $\alpha$  radiation ( $\lambda = 1.54178$  Å) with a special holder to avoid exposure to air during test. The morphologies of the samples were examined using a Hitachi S-4800 field emission scanning electron microscopy (SEM) operated at 5 kV equipped with energy dispersive spectroscopy (EDS). The X-ray photoelectron spectroscopy (XPS) data were collected with a monochromatic Al K $\alpha$  source (1486.6 eV) using a Kratos AXIS Nova Spectrometer. X-ray absorption near edge structure (XANES) measurements were carried out at the Canadian Light Source (CLS). The In L-edge and Cl K-edge XANES spectra were collected using fluorescence yield mode on the soft X-ray micro characterization beamline (SXRMB) at the CLS. To avoid air exposure, all samples were covered with Mylar film attached on Al film and sealed before transforming to the vacuum chamber.

**Conductivity measurements:** Ionic conductivities were measured by AC impedance spectroscopy. Typically, powder samples were placed between two stainless steel rods with 10

mm diameter and pressed at 3 ton (~380 MPa). The thickness of the pellet was between 0.8-1.0 mm depending on the amount of powder samples used. The procedures were performed inside an Ar-filled glovebox. Electrochemical impedance spectroscopy (EIS) was performed with in the temperature range 248-348 K using versatile multichannel potentiostat 3/Z (VMP3) from 7 MHz to 1 Hz with an amplitude of 10 mV. Direct current (DC) polarization measurements were conducted on the pellets with applied voltages of 0.1 V, 0.2 V, 0.3 V, 0.4 V, and 0.5 V for 60 min each to determine the electronic conductivity of the samples.

**Electrochemical Characterizations:** The all-solid-state batteries were fabricated using the prepared annealed- $\text{Li}_3\text{InCl}_6$  SSEs inside the Ar-filled glovebox. The cathode composite incorporating commercial  $\text{LiCoO}_2$  powder without any treatment and the as-prepared  $\text{Li}_3\text{InCl}_6$ . The  $\text{LiCoO}_2$  and  $\text{Li}_3\text{InCl}_6$  were weighed in a weight ratio of 70:30, and then mixed using a pot mill rotator (U.S. Stoneware, No. cz-17018) for 10 min. Annealed- $\text{Li}_3\text{InCl}_6$  was added inside a polytetrafluoroethylene (PTFE) die with diameter of 10 mm), and pressed at 2 ton as SSE layer. Another thin layer of commercial  $\text{Li}_{10}\text{GeP}_2\text{S}_{12}$  (99.95%, MSE supplies, LLC, 10 mg) was further added to avoid the possible influence of redox conversion between  $\text{In}^{3+}$  and In foil (99.99%,  $\Phi$  10 mm, thickness 0.1 mm) anode. The galvanostatic charge-discharge studies of  $\text{LiCoO}_2$  cathodes were conducted with a current density of  $130 \mu\text{A cm}^{-2}$ , within a potential window of 2.5-4.2 V vs.  $\text{Li/Li}^+$  at 25 °C.

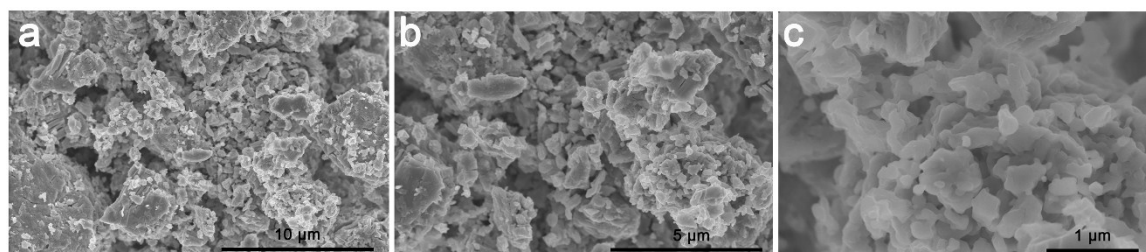


Figure S1. SEM images of ball milled- $\text{Li}_3\text{InCl}_6$  at different magnifications.

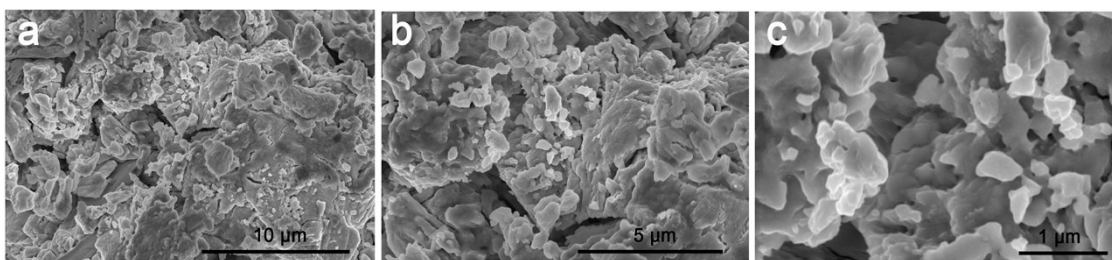


Figure S2. SEM images of annealed-Li<sub>3</sub>InCl<sub>6</sub> at different magnifications.

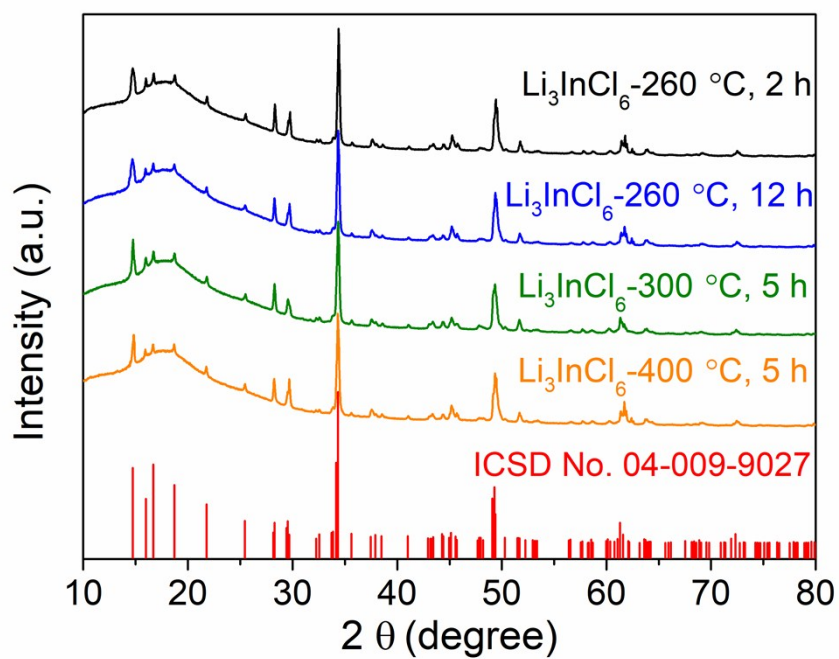


Figure S3. XRD patterns of the annealed-Li<sub>3</sub>InCl<sub>6</sub> samples with different annealing temperatures and durations.

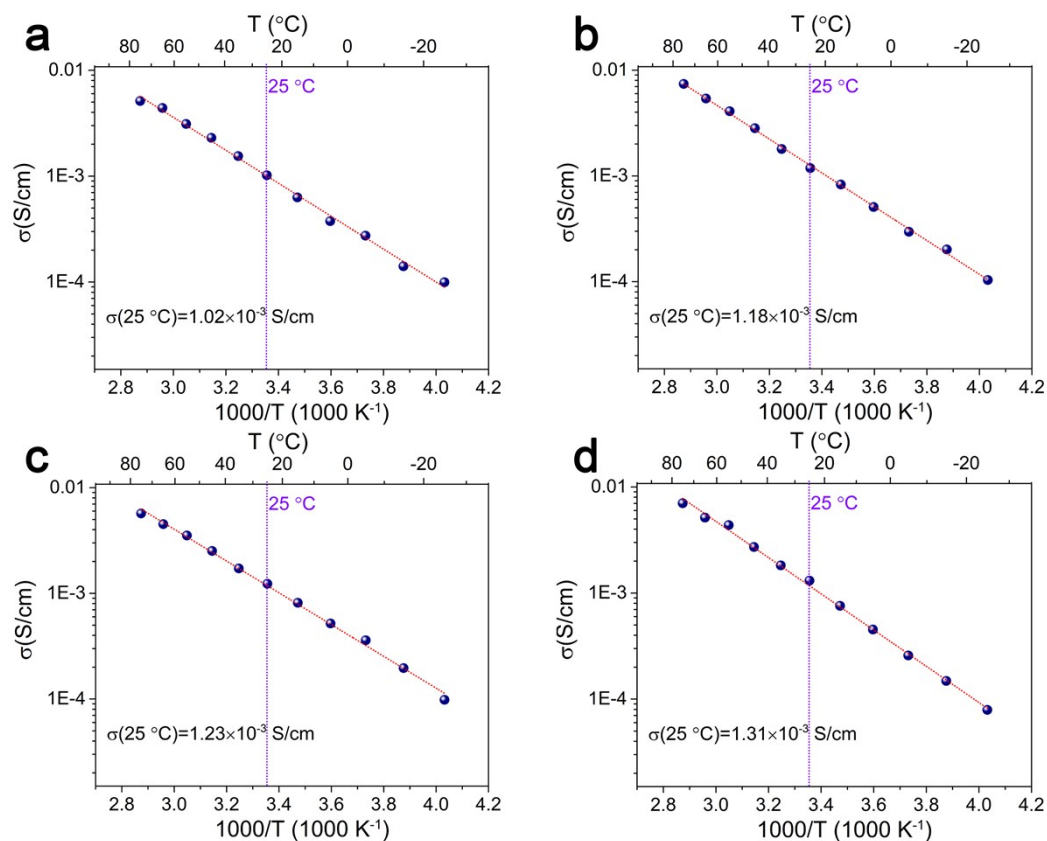


Figure S4. (a-d) Arrhenius plots of the annealed- $\text{Li}_3\text{InCl}_6$  samples with different annealing temperatures and durations.

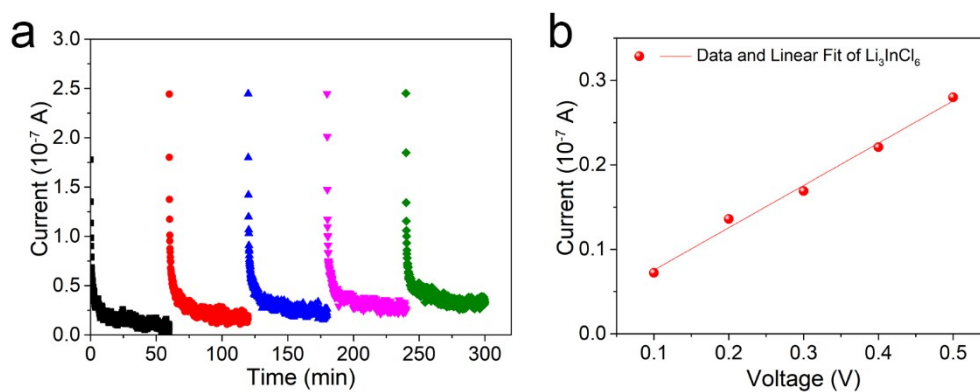


Figure S5. (a) DC polarization curves of annealed- $\text{Li}_3\text{InCl}_6$  using symmetric cell configuration at different voltages from 0.1-0.6 V. (b) Equilibrium current response of annealed- $\text{Li}_3\text{InCl}_6$  symmetric cells at different voltages.

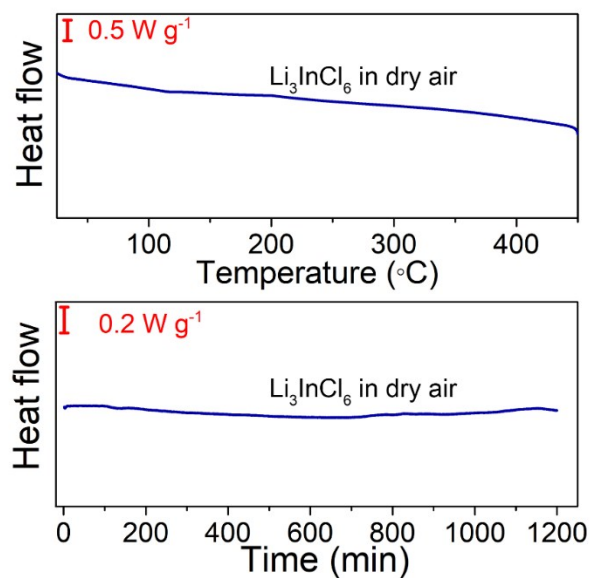


Figure S6. The DSC curves of annealed- $\text{Li}_3\text{InCl}_6$  SSE sample in dry air atmosphere with heating from room temperature to 450 °C at 5 °C  $\text{min}^{-1}$  and resting at room temperature for 20 h.

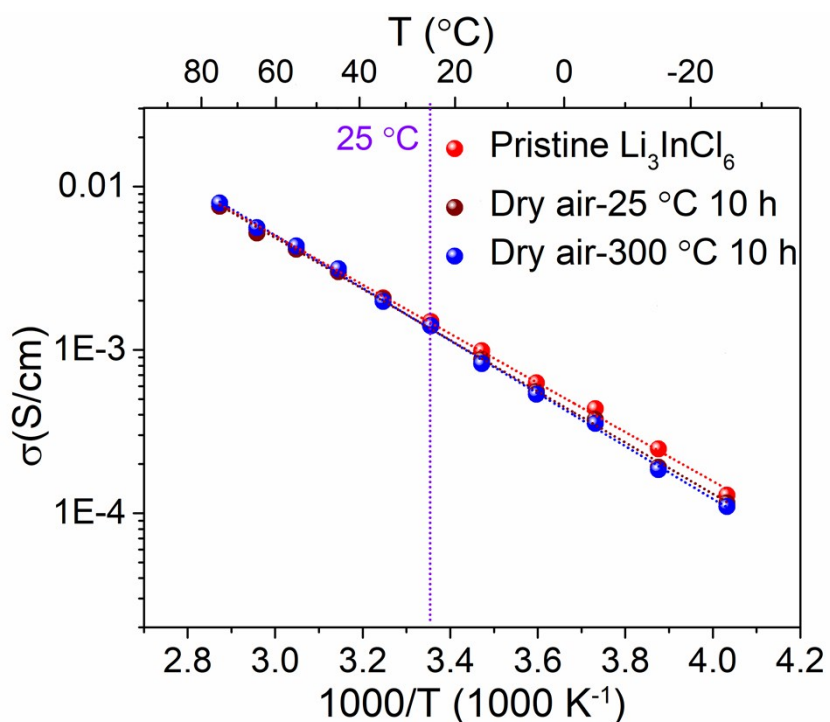


Figure S7. Comparison of ionic conductivities of the pristine annealed- $\text{Li}_3\text{InCl}_6$ , the sample exposure to dry air for 10 h at room temperature, and the sample heated up to 300 °C with heating ratio of 5 °C  $\text{min}^{-1}$  in dry air.

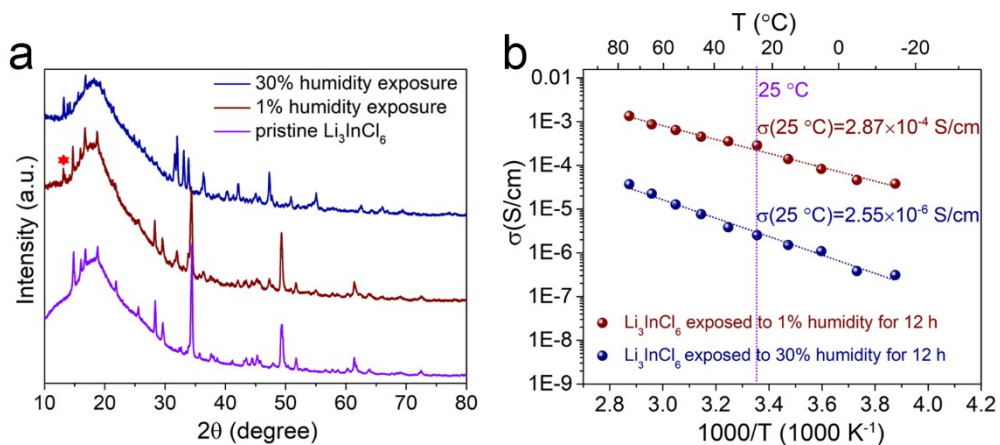


Figure S8. (a) XRD patterns and (b) ionic conductivities of annealed- $\text{Li}_3\text{InCl}_6$  SSE after exposure to air with humidity of 1% and ambient air with humidity around 30% for 12 h.

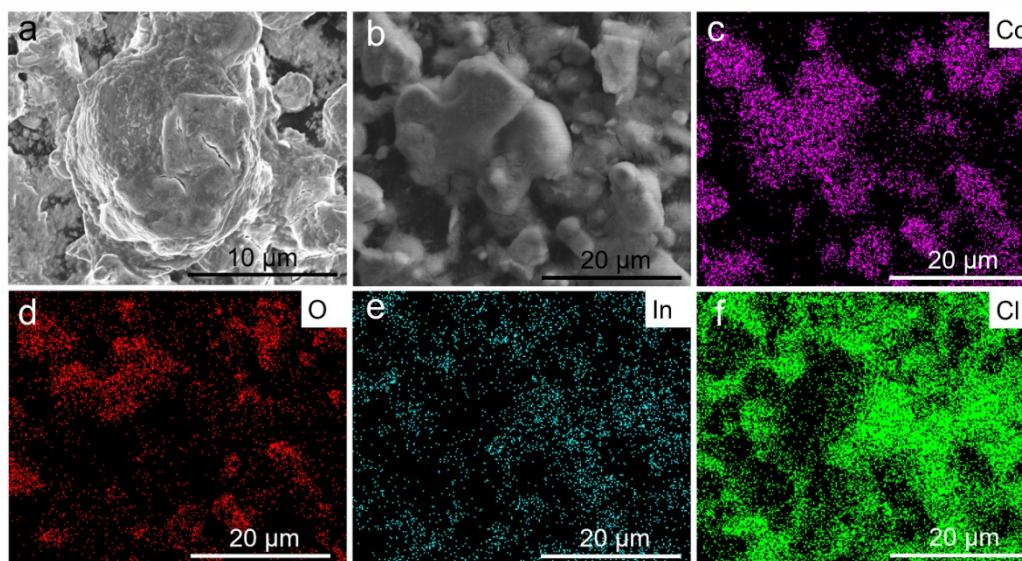


Figure S9. Morphology of  $\text{LiCoO}_2\text{-Li}_3\text{InCl}_6$  composites. (a,b) SEM images at different magnifications and (c-f) corresponding EDX mapping for C, O, In, and Cl elements in (b).

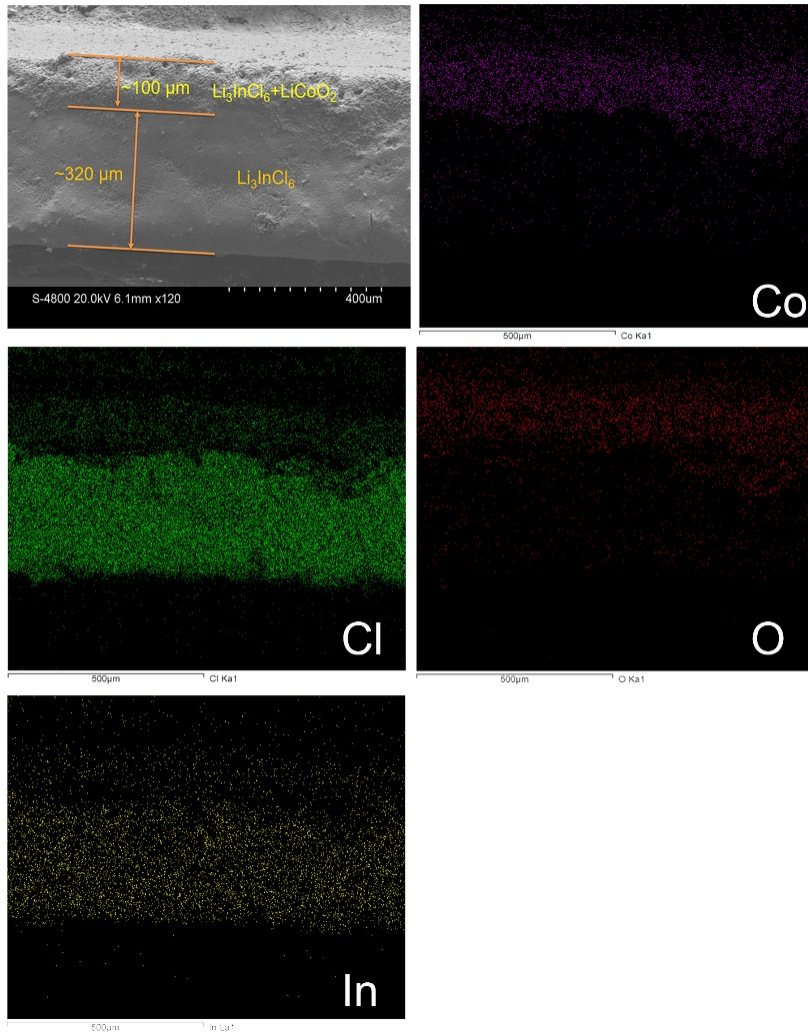


Figure S10. Cross-section view of cathode and  $\text{Li}_3\text{InCl}_6$  SSE layer, and corresponding element distribution.

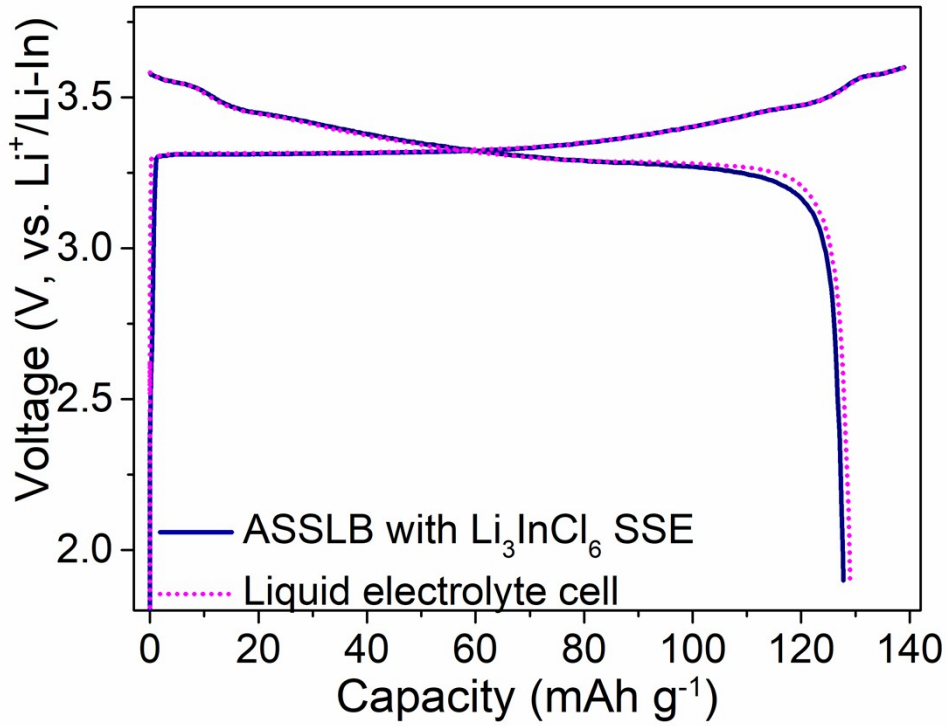


Figure S11. The initial charge-discharge curves of  $\text{LiCoO}_2$  cells at 0.1 C in ASSLB with  $\text{Li}_3\text{InCl}_6$  SSE (solid line) and conventional liquid electrolytes (short dot) based configurations.

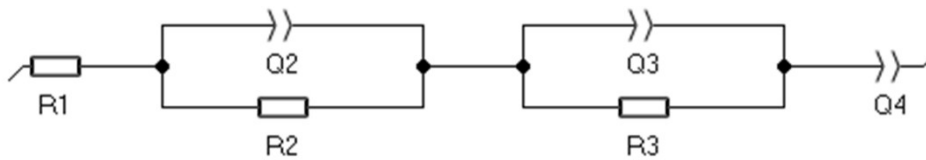


Figure S12. Equivalent circuit of  $R(RQ)(RQ)Q$  for impedance spectra in Figure 3e.

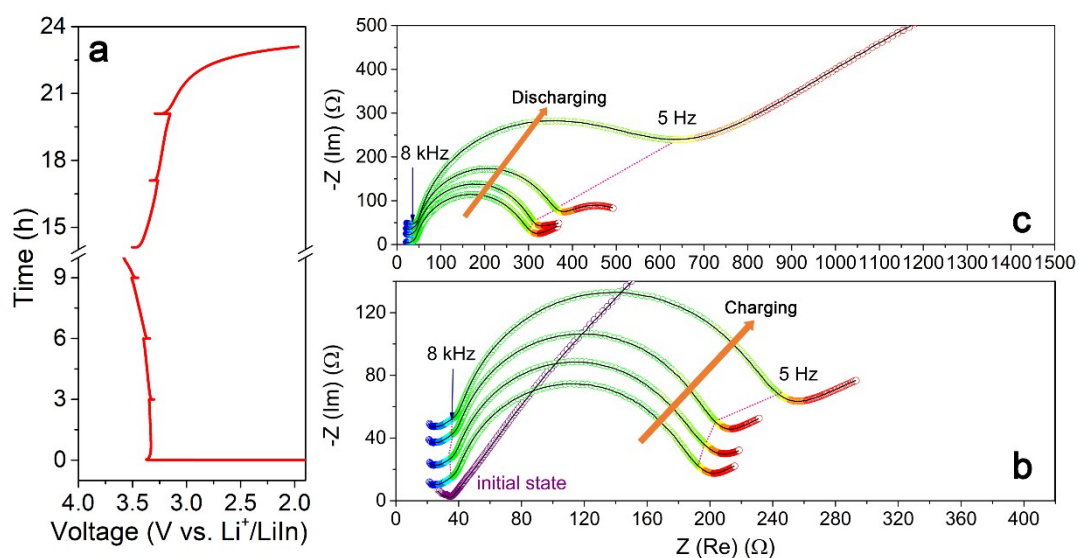


Figure S13. Impedance evolution of all-solid-state LiCoO<sub>2</sub>-In cell with Li<sub>10</sub>GeP<sub>2</sub>S<sub>12</sub> SSE during the first cycle. (A) The charge-discharge curve of ASSLBs with Li<sub>10</sub>GeP<sub>2</sub>S<sub>12</sub> SSE cycled at 0.1 C for 3 h and 2 h rest; (B and C) corresponding impedance spectra recorded after 2 h rest during charging and discharging, respectively.

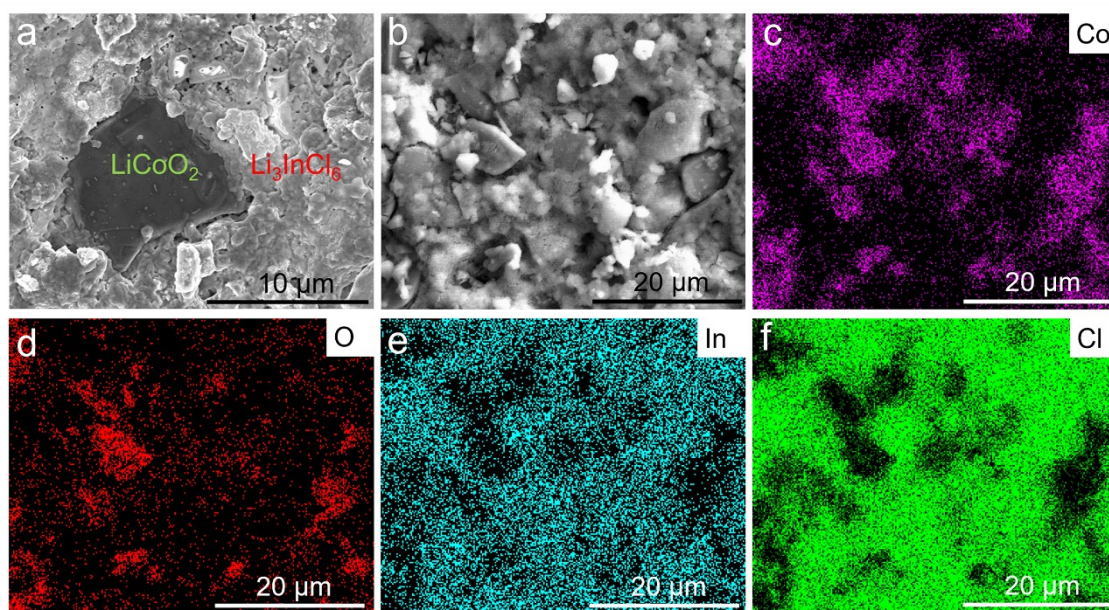


Figure S14. (a,b) SEM images of LiCoO<sub>2</sub>-Li<sub>3</sub>InCl<sub>6</sub> cathode composites at fully charged state, and (c-f) corresponding EDX mapping for Co, O, In, and Cl elements in (b).

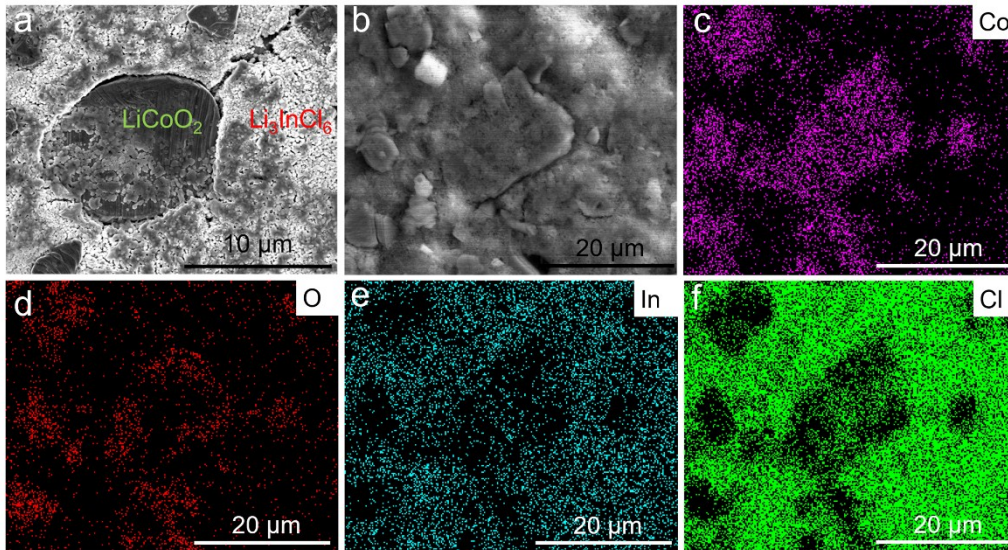


Figure S15. (a,b) SEM images of  $\text{LiCoO}_2\text{-Li}_3\text{InCl}_6$  cathode composites at fully discharged state, and (c-f) corresponding EDX mapping for Co, O, In, and Cl elements in (b).

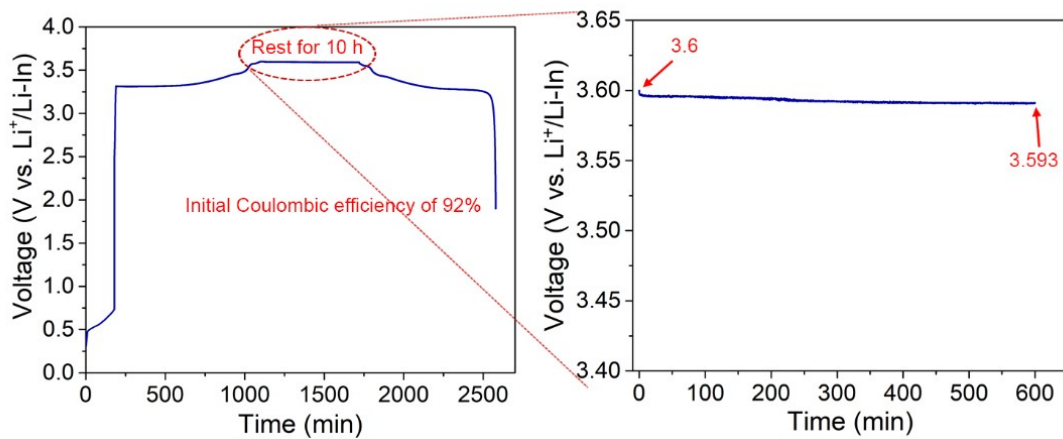


Figure S16. The open circuit voltage stability (OCV) vs. time at 100% SOC (fully charged state).

Table S1. Ionic conductivities of reported halide SSEs.

Halide SSEs	Ionic conductivity (S cm <sup>-1</sup> )	Phase transition	Ref.
Li <sub>2</sub> ZnCl <sub>4</sub>	3×10 <sup>-4</sup> (300 °C)	phase transition at 215 °C	[1]
Li <sub>6</sub> FeCl <sub>8</sub>	2×10 <sup>-3</sup> (200 °C)	phase transition at 300 °C	[2]
Li <sub>2</sub> MnCl <sub>4</sub>	1.8×10 <sup>-4</sup> (100 °C)	phase transition at 355 °C	[3]
Li <sub>2</sub> CdCl <sub>4</sub>	2.1×10 <sup>-4</sup> (100 °C)	phase transition at 345 °C	[3]
Li <sub>2</sub> MnBr <sub>4</sub>	1×10 <sup>-4</sup> (100 °C)	-	[3]
Li <sub>4</sub> PbI <sub>6</sub>	1.7×10 <sup>-4</sup> (197 °C)	phase transition at 267 °C	[4]
Li <sub>2</sub> PbI <sub>4</sub>	3×10 <sup>-5</sup> (197 °C)	phase transition at 267 °C	[4]
LiInBr <sub>4</sub>	~10 <sup>-7</sup> at 25 °C as prepared 1×10 <sup>-3</sup> at 25 °C (High-temperature phase)	phase transition at 43 °C and -13 °C	[5]
Li <sub>3</sub> InBr <sub>6</sub>	~10 <sup>-7</sup> at 25 °C as prepared 1×10 <sup>-3</sup> at 25 °C (High-temperature phase)	phase transition at 41 °C and -13 °C	[5-6]
Li <sub>3</sub> InBr <sub>6-x</sub> Cl <sub>x</sub> with x≤4	1.2×10 <sup>-4</sup> at 27 °C	phase transition at 12 °C	[7]
Li <sub>3</sub> InBr <sub>6-y</sub> X <sub>y</sub> (X=F, I)	3×10 <sup>-3</sup> at 60 °C for Li <sub>3</sub> InBr <sub>3</sub> I <sub>3</sub> Others <10 <sup>-5</sup> at 25 °C	phase transition at 60 °C	[8]
Li <sub>3-2x</sub> Mg <sub>x</sub> InBr <sub>6</sub> (x= 0.02-0.4)	<10 <sup>-5</sup> at 25 °C	phase transition at ~37-57 °C	[9]
Li <sub>3-2x</sub> M <sub>x</sub> InBr <sub>6</sub> (M=Mg, Ca, Sr, Ba; x=0-1.0)	2×10 <sup>-5</sup> at 25 °C for Li <sub>2</sub> Ba <sub>0.5</sub> InBr <sub>6</sub> , Others <10 <sup>-5</sup> at 25 °C	phase transition at ~37-57 °C for Mg or Sc compounds, ~111 °C for Ca compound	[10]
LiInI <sub>4</sub>	~10 <sup>-8</sup> (25 °C)		[11]

Table S2. Ionic conductivities and corresponding activation energies of annealed-Li<sub>3</sub>InCl<sub>6</sub> SSE and after air exposure.

Samples	Ionic conductivity at 25 °C (mS cm <sup>-1</sup> )	Ionic conductivity retention	Activation energy (eV)
Pristine Li <sub>3</sub> InCl <sub>6</sub>	1.49	-	0.326
Reheated Li <sub>3</sub> InCl <sub>6</sub> after 1% humidity exposure	1.37	91.9%	0.335
Reheated Li <sub>3</sub> InCl <sub>6</sub> after ambient air exposure	1.35	90.6%	0.332
Li <sub>3</sub> InCl <sub>6</sub> exposed in dry air at 25°C for 10 h	1.41	94.6%	0.336
Li <sub>3</sub> InCl <sub>6</sub> exposed dry air at 300°C for 10 h	1.4	94.0%	0.345

- [1] H. D. Lutz, K. Wussow, P. Kuske, *Zeitschrift für Naturforschung B* **1987**, *42*, 1379-1386.
- [2] R. Kanno, Y. Takeda, M. Mori, O. Yamamoto, *Chemistry Letters* **1987**, *16*, 1465-1468.
- [3] W. Schmidt, H. Lutz, *Berichte der Bunsengesellschaft für physikalische Chemie* **1984**, *88*, 720-723.
- [4] H. Lutz, Z. Zhang, A. Pfitzner, *Solid state ionics* **1993**, *62*, 1-3.
- [5] K. Yamada, K. Kumano, T. Okuda, *Solid state ionics* **2006**, *177*, 1691-1695.
- [6] Y. Tomita, H. Ohki, K. Yamada, T. Okuda, *Solid state ionics* **2000**, *136*, 351-355.
- [7] Y. Tomita, H. Matsushita, K. Kobayashi, Y. Maeda, K. Yamada, *Solid State Ionics* **2008**, *179*, 867-870.

- [8] Y. Tomita, H. Nishiyama, K. Kobayashi, Y. Kohno, Y. Maeda, K. Yamada, *ECS Transactions* **2009**, *16*, 137-141.
- [9] Y. Tomita, H. Yonekura, Y. Yamauchi, K. Yamada, K. Kobayashi, *Zeitschrift für Naturforschung A* **2002**, *57*, 447-450.
- [10] Y. Tomita, H. Matsushita, H. Yonekura, Y. Yamauchi, K. Yamada, K. Kobayashi, *Solid state ionics* **2004**, *174*, 35-39.
- [11] K. Yamada, S. Matsuyama, Y. Tomita, Y. Yamane, *Solid State Ionics* **2011**, *189*, 7-12.